The Effect of Imperfect Carrier Frequency Offset Estimation on an OFDMA Uplink

Zhongshan Zhang, *Member, IEEE,* and Chintha Tellambura, *Senior Member, IEEE*

***Abstract*—In the uplink of Orthogonal Frequency-Division Multiple Access (OFDMA) systems, the user carrier frequency offsets result in inter-carrier-interference (ICI) and multiple-user-interference (MUI), leading to a degradation of the bit error rate (BER). This paper treats this uplink scenario and derives the average uplink capacity and the BER using the signal-to-interference-and-noise ratio (SINR) analysis. Adaptive power allocation is suggested to increase the capacity. When the frequency offsets are modeled as zero-mean Gaussian or Uniform random variables, the BER is derived as a closed-form infinite-series. The series requires at least 50 terms to ensure sufficient accuracy.**

***Index Terms*—Carrier frequency offset, bit error rate, OFDMA.**

I. INTRODUCTION

IN the Orthogonal Frequency-Division Multiple Access (OFDMA) uplink [1]–[3], different users may have different carrier frequency offsets, which results in multiple-user-interference (MUI). Moreover, frequency offsets also cause inter-carrier-interference (ICI). For example, the bit error rate (BER) of OFDM systems impaired by carrier frequency offset is analyzed in [4]. Although several high-performance classical frequency offset and channel estimators are available [5], [6], the interference degrades their performance, and they may require a large overhead of pilot symbols [7]. MUI cancellation in OFDMA system is discussed in [8], where MUI cancellation requires knowledge of the carrier frequency offsets.

In this paper, the effect of the frequency offset on the OFDMA uplink is analyzed in detail. Although the interference analysis for this case has been studied previously [1], a compact representation of signal-to-interference-and-noise ratio (SINR) as a function of the frequency offset variance is not given in [1]. Therefore, the average SINR of each user and an adaptive power allocation scheme to improve the uplink capacity are derived. Based on the SINR analysis, the BER of the OFDMA uplink degraded by the carrier frequency offset is also derived. Using the BER result in [9, Eq.(17)], an infinite BER series is derived when the frequency offset is a zero-mean Gaussian or Uniform random variable (RV). Truncation of the series to about 50 terms yields high accuracy.

Paper approved by C. Tepedelenlioglu, the Editor for Synchronization and Equalization of the IEEE Communications Society. Manuscript received May 25, 2007; revised February 20, 2008 and August 26, 2008.

The authors are with the Department of Electrical and Computer Engineering, University of Alberta, Edmonton, AB T6G 2V4, Canada (e-mail: {zszhang, chintha}@ece.ualberta.ca).

This paper was presented in part at IEEE ICC2007.
Digital Object Identifier 10.1109/TCOMM.2009.04.070246

The remainder of this paper is organized as follows. The OFDMA system model is described in Section II, and the ergodic capacity of the OFDMA uplink with the carrier frequency offset is derived in Section III. The BER degradation due to frequency offsets is analyzed in Section IV. Conclusions are provided in Section V.

Notation: $(\cdot)^H$ denotes conjugate transpose. The imaginary unit is $\jmath = \sqrt{-1}$. A real Gaussian variable with mean a and variance σ^2 is denoted by $x \sim \mathcal{N}(a, \sigma^2)$. A circularly symmetric complex Gaussian variable with mean m and variance σ_w^2 is denoted by $w \sim \mathcal{CN}(m, \sigma_w^2)$. $\mathbb{E}\{x\}$ denotes the mean of x. $\mathbf{F}$ denotes the $N \times N$ Inverse Discrete Fourier Transform (IDFT) matrix with $[\mathbf{F}]_{nk} = \frac{1}{\sqrt{N}} e^{\frac{\jmath 2\pi nk}{N}}$ for $0 \le n, k \le N-1$.

II. OFDMA UPLINK SIGNAL MODEL

An OFDMA uplink with K users is considered, with the total number of subcarriers being N. An $N \times 1$ vector $\tilde{\mathbf{X}}_k$ represents the symbols transmitted by the k-th user, where $k \in \{1, 2, \cdots, K\}$. The i-th entry of $\tilde{\mathbf{X}}_k$ (i.e., $\tilde{\mathbf{X}}_k[i]$) is nonzero if and only if the $i \in G_k$. G_k is the subcarrier group allocated to the k-th user (the elements of G_k are indexes of all those subcarriers), and $\mathcal{N}_k$ represents the cardinality of G_k. Note that $\bigcap_{k \neq l} G_k G_l = \emptyset$ and $\bigcup_{k=1}^{K} G_k \subseteq \{0, 1, \cdots, N-1\}$. These entries are complex data symbols from a signal constellation such as M-ary phase-shift keying (PSK) or M-ary quadrature amplitude modulation (QAM). $\tilde{\mathbf{X}}_k$ can also be simplified into an $\mathcal{N}_k \times 1$ vector $\mathbf{X}_k$ by deleting all the zero entries of $\tilde{\mathbf{X}}_k$.

The time-domain transmit vector of the k-th user is given by $\bar{\mathbf{s}}_k = \mathbf{F}\tilde{\mathbf{X}}_k = \mathbf{F}_k \mathbf{X}_k$, where $\mathbf{F}_k$ is the $N \times \mathcal{N}_k$ IDFT matrix that is specified by G_k (by deleting all the columns that are not in G_k from $\mathbf{F}$). A length-N_g cyclic prefix (CP) is used.

The discrete-time channel impulse response of the k-th user is $\mathbf{h}_k = [h_k(0), h_k(1), \cdots, h_k(L_k - 1)]^T$, where L_k is the maximum delay of the k-th user. The frequency-domain channel attenuation matrix of the k-th user is given by $\mathbf{H}_k = \text{diag}\{H_k[i] : i \in G_k\}$, which is an $\mathcal{N}_k \times \mathcal{N}_k$ diagonal matrix with its diagonal entries equal to $H_k[i] = \sum_{n=0}^{L_k-1} h_k(n) e^{-\frac{\jmath 2\pi ni}{N}}$, $i \in G_k$. The received signal at the base station can be represented as

$$\mathbf{y} = \sum_{k=1}^{M} \mathbf{E}_k \mathbf{F}_k \mathbf{H}_k \mathbf{\Phi}_k \mathbf{X}_k + \mathbf{w}, \tag{1}$$

where $\mathbf{\Phi}_k = \text{diag}\left\{\sqrt{P_i} : i \in G_k\right\}$ is an $\mathcal{N}_k \times \mathcal{N}_k$ diagonal matrix to P_i, $i \in G_k$ is the power allocated to the i-th subcarrier of the k-th user, and $\mathbf{E}_k$, an $N \times N$ diagonal matrix, is given by $\mathbf{E}_k = \operatorname{diag}\left\{e^{\jmath\psi_k}, e^{\jmath\left(\frac{2\pi\varepsilon_k}{N}+\psi_k\right)}, \cdots, e^{\jmath\left(\frac{2\pi\varepsilon_k\times(N-1)}{N}+\psi_k\right)}\right\}$ with ψ_k and ε_k representing the initial phase and the normalized frequency offset (the frequency offset normalized to the subcarrier spacing) of the k-th user, respectively. Frequency offsets ε_k, $k = 1, \cdots, K$, are independent and identically distributed (i.i.d.) random variables with mean zero and variance of σ_ϵ^2 (not necessarily Gaussian). The noise vector $\mathbf{w}$ is additive white Gaussian noise (AWGN) with $\mathbf{w}[i] \sim \mathcal{CN}(0, \sigma_w^2)$.

Data recovery for user k requires Discrete Fourier Transform (DFT) demodulation given by $\hat{\mathbf{X}} = \mathbf{F}_k^H\mathbf{y}$. However, since the frequency offsets destroy the orthogonality among the users, and the resulting SINR degrades $\hat{\mathbf{X}}$. By using $\gamma_{m|m\in G_k}$ to represent the SINR of user k at the m-th subcarrier, from the interference analysis in [10], the average SINR of user k can be approximated as

$$\begin{aligned}\mathrm{SINR}_k &= \mathbb{E}\left\{\gamma_{m|m\in G_k}\right\} \\ &= \frac{\mathrm{SNR}_k}{\frac{\pi^2\sigma_\epsilon^2\mathrm{SNR}_k}{3}+1}\cdot\left(1-\frac{\pi^2\sigma_\epsilon^2}{3}+\frac{\pi^4\sigma_\epsilon^4}{20}\right).\end{aligned} \tag{2}$$

III. Ergodic Capacity of OFDMA Uplink with Carrier Frequency Offset

This section analyzes the OFDMA uplink capacity in the presence of frequency offsets. A quasi-static wireless channel is assumed (i.e., the channel is constant for one OFDM symbol but may vary for the next). Both ergodic capacity and outage capacity are common performance metrics [11, chapter 5]. For brevity, only the ergodic capacity is analyzed in this letter.

For OFDMA systems with a total of K users, the ergodic capacity in a frequency-selective fading channel can be defined as [11, page 182]:

$$\begin{aligned}\mathbb{C}_U = &\max_{\substack{G_1,\cdots,G_M,\\ P_0,\cdots,P_{N-1}}}\sum_{i=0}^{N-1}\log(1+\gamma_i) \quad (\text{bits/OFDMA symbol}),\\ &s.t. \quad \sum_{m\in G_k}\log(1+\gamma_m)\geq R_k \quad 1\leq k\leq K,\\ &\qquad \sum_{m\in G_k}P_m = \mathcal{N}_k\bar{P}_k \qquad 1\leq k\leq K,\end{aligned} \tag{3}$$

where γ_m is the SINR of subcarrier m and R_k and $\bar{P}_k$ are the rate of reliable communication and the averaged power constraint for user k, respectively.

Water-filling power allocation solves (3) readily [11]. We apply the same algorithm in the presence of frequency offsets. The water-filling power allocation for the m-th subcarrier of user k is then given by:

$$P_{m\in G_k}^* = \left(\frac{1}{\lambda_k} - \frac{\frac{\pi^2\sigma_\epsilon^2\kappa_m}{3}+\sigma_w^2}{|H_k[m]|^2\frac{\sin^2(\pi\varepsilon_k)}{N^2\sin^2\left(\frac{\pi\varepsilon_k}{N}\right)}}\right)^+ \quad 1\leq k\leq K, \tag{4}$$

where $\sum_{k=1}^{K}\left(\lambda_k\sum_{m\in G_k}P_{m\in G_k}^*\right) = \sum_{k=1}^{K}\mathcal{N}_k\bar{P}_k$ and $\kappa_m =$

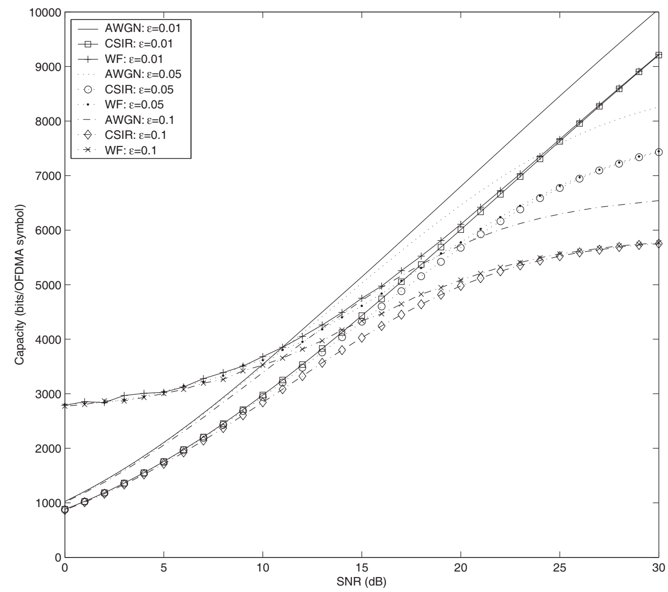

Fig. 1. OFDMA uplink capacity with non-zero carrier frequency offset.

$\mathbb{E}\left\{\left|\sqrt{P_i}H_m[i]\right|^2\right\}$. Therefore the uplink capacity is

$$\begin{aligned}&\mathbb{C}_{U|WF}\\ &= \sum_{k=1}^{K}\sum_{m\in G_k}\mathbb{E}\left\{\log\left(1+\frac{P_m|H_k[m]|^2\frac{\sin^2(\pi\varepsilon_k)}{N^2\sin^2\left(\frac{\pi\varepsilon_k}{N}\right)}}{\frac{\pi^2\sigma_\epsilon^2\kappa_m}{3}+\sigma_w^2}\right)\right\}.\end{aligned} \tag{5}$$

Note that the water-filling power allocation requires the knowledge of both the channel state information and the frequency offset. In this paper, uplink parameter estimation is assumed, i.e., both the channel and the frequency offset of each user should be estimated at the base station, and the estimation results will be forwarded to each user through the downlink signalling.

Fig. 1 illustrates the ergodic capacity of the OFDMA uplink with the carrier frequency offset and $N = 1024$. For comparison purpose, for a frequency-selective fading channel with channel state information at the receiver (CSIR), we have $\mathbb{C}_{U|CSIR} \cong N \cdot \log_2^e \cdot \mathbb{E}\{\gamma_i\}$ in the low SINR scenario, or $\mathbb{C}_{U|CSIR} \cong N\cdot\mathbb{E}\{\log(\gamma_i)\}$ in the high SINR case [11]. Note that the uplink capacity for an AWGN channel is $\mathbb{C}_{U|AWGN} = \sum_{i=0}^{N-1}\log(1+\mathrm{SNR}_i)$. Fig. 1 shows the effectiveness of water-filling power allocation. For example, for an SNR of 20 dB and with CSIR, without water-filling power allocation, uplink ergodic capacities of 6000, 5700, and 5000 (bits/symbol) can be achieved when $\sigma_\epsilon^2 = 3.3\times10^{-5}$, $\sigma_\epsilon^2 = 8.3\times10^{-4}$ and $\sigma_\epsilon^2 = 3.3\times10^{-3}$, respectively. With water-filling power allocation, the uplink capacities will be about 6100, 5800 and 5100 (bits/symbol), respectively; i.e., an improvement of about 100 (bits/symbol) is achieved for each scenario.

IV. BER Analysis

This section analyses the BER as a function of SINR for the OFDMA uplink. M-ary square QAM with Gray bit-mapping is considered. As before, the quasi-static channel is assumed.

The BER for square QAM without considering the frequency offset is discussed in [9]. In [6], the BER is evaluated for synchronization and channel estimation errors.

Here the BER is derived as an infinite series, when the frequency offset is a Gaussian or Uniformly distributed RV. Unlike [6], only the effect of frequency offset on the BER is analyzed, and perfect channel knowledge is assumed. The averaged BER is given by [9]:

$$P_{BER}^{M} = \mu_1(M) \cdot \mathbb{E}\left\{\text{erfc}\left(\sqrt{3\mu_3(M)\cdot\gamma_{m|m\in G_k}}\right)\right\} + \mu_2(M)\cdot\mathbb{E}\left\{\text{erfc}\left(3\sqrt{3\mu_3(M)\cdot\gamma_{m|m\in G_k}}\right)\right\}, \tag{6}$$

where $\mu_1(M) = \frac{\sqrt{M}-1}{\sqrt{M}\log_2\sqrt{M}}$, $\mu_2(M) = \frac{\sqrt{M}-2}{\sqrt{M}\log_2\sqrt{M}}$, $\mu_3(M) = \frac{\log_2 M}{2(M-1)\log_2^M}$, $\text{erfc}(x) = \frac{2}{\sqrt{\pi}}\int_x^\infty e^{-u^2}\text{d}u$, and the expectation is with respect to $\gamma_{m|m\in G_k}$. Closed-form P_{BER}^M appears intractable.

Here the first case that is analyzed is that the frequency offset of each user is an i.i.d. RV that is uniformly distributed in $(-\epsilon,\epsilon)$. From [12, page 939], $\text{erfc}\left(\sqrt{3\mu_3(M)\cdot\gamma_{m|m\in G_k}}\right)$ as well as $\text{erfc}\left(3\sqrt{3\mu_3(M)\cdot\gamma_{m|m\in G_k}}\right)$ can be represented as an infinite series and, therefore, P_{BER}^M is given by

$$\begin{aligned}
P_{BER}^{M} &= \frac{2\sqrt{M}-3}{\sqrt{M}\log_2\sqrt{M}} - \frac{2\sqrt{6}(\sqrt{M}-1)}{\pi\epsilon\log_2\sqrt{M}\sqrt{M\pi\bar{\mathcal{J}}^M}}\sum_{n=1}^{\infty}\beta_{1,n}^M \\
&\quad - \frac{2\sqrt{6}(\sqrt{M}-2)}{\pi\epsilon\log_2\sqrt{M}\sqrt{M\pi\bar{\mathcal{J}}^M}}\sum_{n=1}^{\infty}\beta_{2,n}^M \\
&= \frac{2\sqrt{M}-3}{\sqrt{M}\log_2\sqrt{M}} - \frac{2\sqrt{6}(\sqrt{M}-1)}{\pi\epsilon\log_2\sqrt{M}\sqrt{M\pi\bar{\mathcal{J}}^M}}\sum_{n=1}^{\infty}\beta_{1,n}^M \\
&\quad - \frac{2\sqrt{6}(\sqrt{M}-2)\beta_{2,1}^M}{\pi\epsilon\log_2\sqrt{M}\sqrt{M\pi\bar{\mathcal{J}}^M}} \\
&\quad - \frac{2\sqrt{6}(\sqrt{M}-2)}{\pi\epsilon\log_2\sqrt{M}\sqrt{M\pi\bar{\mathcal{J}}^M}}\sum_{n=1}^{\infty}3^{2n+1}\beta_{1,n}^M \\
&= \frac{2\sqrt{M}-3}{\sqrt{M}\log_2\sqrt{M}} - \frac{2\sqrt{6}(\sqrt{M}-2)\beta_{2,1}^M}{\pi\epsilon\log_2\sqrt{M}\sqrt{M\pi\bar{\mathcal{J}}^M}} \\
&\quad - \frac{2\sqrt{6}}{\pi\epsilon\log_2\sqrt{M}\sqrt{M\pi\bar{\mathcal{J}}^M}} \\
&\quad \cdot \sum_{n=1}^{\infty}\left(\left(3^{2n+1}+1\right)\sqrt{M} - 2\cdot 3^{2n+1} - 1\right)\beta_{1,n}^M,
\end{aligned} \tag{7}$$

where $\beta_{1,n}^M = \frac{(-1)^{n+1}}{(2n-1)(n-1)!}\int_0^{\pi\epsilon\sqrt{\frac{\bar{\mathcal{J}}^M}{6}}}(\bar{\mathcal{J}}^M - y^2)^{2n-1}\text{d}\,y$, $\beta_{2,n}^M = \frac{(-1)^{n+1}3^{2n-1}}{(2n-1)(n-1)!}\int_0^{\pi\epsilon\sqrt{\frac{\bar{\mathcal{J}}^M}{6}}}(\bar{\mathcal{J}}^M - y^2)^{2n-1}\text{d}\,y$ and $\bar{\mathcal{J}}^M = \sqrt{3\mu_3(M)\times\frac{9\text{SNR}}{\pi^2\epsilon^2\text{SNR}+9}}$. The following recursive

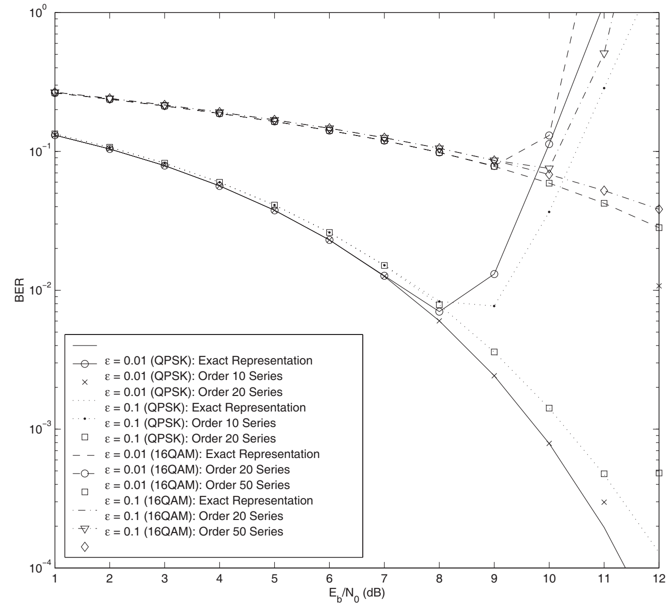

Fig. 2. The approximation of BER with finite order series.

relationships hold:

$$\begin{aligned}
\beta_{1,n}^M &= a_n^M + b_n^M - \frac{8(2n-3)\bar{\mathcal{J}}^{M\,2}}{(4n-1)(4n-3)}\cdot\beta_{1,n-1}^M \\
&= \frac{(-1)(2n-3)(4n-5)\left(\bar{\mathcal{J}}^M - \frac{\pi^2\epsilon^2\bar{\mathcal{J}}^M}{6}\right)^2}{(n-1)(2n-1)(4n-1)}\cdot a_{n-1}^M \\
&\quad + \frac{(-1)(4n-5)(4n-7)\left(\bar{\mathcal{J}}^M - \frac{\pi^2\epsilon^2\bar{\mathcal{J}}^M}{6}\right)^2}{(n-1)(4n-1)(4n-3)}\cdot b_{n-1}^M \\
&\quad - \frac{8(2n-3)\bar{\mathcal{J}}^{M\,2}}{(4n-1)(4n-3)}\cdot\beta_{1,n-1}^M,
\end{aligned} \tag{8}$$

and

$$\beta_{2,n}^M = 3^{2n-1}\beta_{1,n-1}^M, \tag{9}$$

as derived in Appendix A. Given the initial condition of $a_1^M = \frac{\pi\epsilon\sqrt{\frac{\bar{\mathcal{J}}^M}{6}}\left(\bar{\mathcal{J}}^M - \frac{\pi^2\epsilon^2\bar{\mathcal{J}}^M}{6}\right)}{3}$, $b_1^M = \frac{2\pi\epsilon\bar{\mathcal{J}}^M\sqrt{\frac{\bar{\mathcal{J}}^M}{6}}}{3}$, $\beta_{1,1}^M = \left(\pi\epsilon - \frac{\pi^3\epsilon^3}{18}\right)\bar{\mathcal{J}}^M\sqrt{\frac{\bar{\mathcal{J}}^M}{6}}$ and $\beta_{2,1}^M = 3\left(\pi\epsilon - \frac{\pi^3\epsilon^3}{18}\right)\bar{\mathcal{J}}^M\sqrt{\frac{\bar{\mathcal{J}}^M}{6}}$, the coefficients $a_{n>1}^M$, $b_{n>1}^M$, $\beta_{1,n>1}^M$ and $\beta_{2,n>1}^M$ can be easily generated.

The average BER can also be expressed as an infinite series when the frequency offsets are modeled as zero-mean Gaussian RVs, i.e., $\varepsilon_k \sim \mathcal{N}(0,\sigma_\epsilon^2)$. Given the initial conditions of $\mathcal{D}_0^M = 1$, $\mathcal{D}_1^M = 1 - \frac{\pi^2\sigma_\epsilon^2}{6}$ and $\mathcal{D}_2^M = 1 - \frac{\pi^2\sigma_\epsilon^2}{3} + \frac{\pi^4\sigma_\epsilon^4}{12}$, P_{BER}^M as an infinite series is derived in Appendix B. However, in our analysis, for brevity, a uniform distribution instead of a Gaussian distribution is used.

However, in practice, the infinite series for P_{BER}^M must be truncated to approximate (6). The impact of this truncation is investigated in Fig. 2, where the BER is plotted as a function

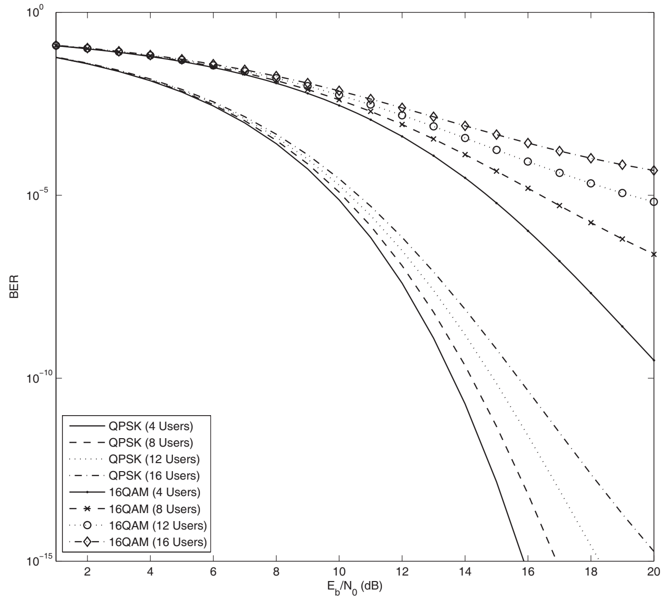

Fig. 3. BER as a function of number of accessing users.

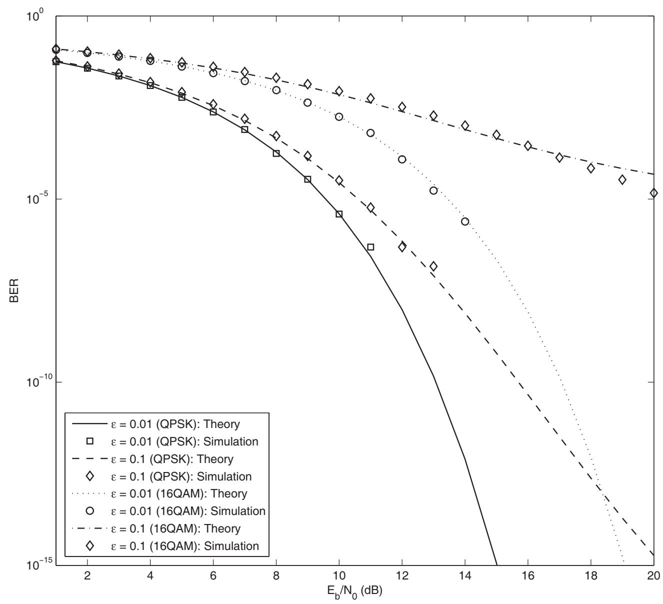

Fig. 4. BER with non-zero carrier frequency offset.

of $\frac{E_b}{N_0}$ (energy power bit per noise power density). The number of terms (order) in (7) required to converge to (6) are shown. With a small order, (7) approximates P_{BER}^M for at low SNR, and the truncated series expression breaks down as the SNR increases. This breakdown appears earlier for a smaller ϵ (or σ_ϵ^2). For example, consider the case that the user frequency offsets are uniformly distributed in $(-\epsilon, \epsilon)$, and each subcarrier is modulated by 4-phase PSK (QPSK). When the frequency offset is 1% and for an order of 10, (7) converges at P_{BER}^M only when SNR $\leq$7 dB. With 10% frequency offset, this convergence can be achieved well until SNR=8 dB. A similar convergence performance also holds for high-order modulation, e.g., 16QAM. This deviation at a high SNR can be mitigated by increasing the order. For example, by increasing the order to 50, (7) with each modulation converges at P_{BER}^M well at SNR=10 dB for each evaluated ϵ.

The BER as a function of the number of users is illustrated in Fig. 3 for $N = 1024$ and 10% frequency offset. Each user is allocated 64 subcarriers with an interleaved subcarrier allocation. The maximum number of users is 16. The BER increases when a larger number of users accessing the base station, for both QPSK and 16QAM. For example, with QPSK, the performance gap between the 4-user case and the 16-user case is about 4.5 dB, and that gap for 16QAM is about 6.1 dB.

The BER losses due to the carrier frequency offset are shown in Fig. 4, where the number of users is 16 and the number of subcarriers per user is 64. Subcarrier modulation either QPSK or 16QAM (Gray bit mapping). Increasing frequency offsets degrade the BER regardless of the modulation format. For example, with QPSK, the performance degrades by about 5.2 dB at high SNR when the frequency offset increases from 1% to 10%. The corresponding loss for 16QAM is 7.3 dB at high SNR. For a smaller frequency offset (1%), the simulation result matches the theoretical analysis well, but a deviation occurs at high SNR for a larger frequency offset (10%). For the same SINR, since the effective $\frac{E_b}{N_0}$ in 16QAM is much lower than that in QPSK, the BER for 16QAM is much higher than that for the latter.

V. Conclusions

The OFDMA-uplink BER degradation due to the carrier frequency offset has been derived as a function of SINR. The ergodic capacity of OFDMA uplink with carrier frequency offset has been derived with water-filling power allocation. When the frequency offset is modeled as a zero-mean uniform or Gaussian RV, the BER expression is an infinite series. The series can be truncated with negligible error.

Appendix A
BER with Uniform Frequency Offsets

In order to derive the averaged BER, we first derive the PDF of z_k^M given by

$$\begin{aligned} z_k^M &= \sqrt{3\mu_3(M)\cdot\gamma_{m|m\in G_k}} \\ &= \underbrace{\sqrt{3\mu_3(M)\cdot\frac{9\mathrm{SNR}_k}{\pi^2\epsilon^2\mathrm{SNR}_k+9}}}_{J_k^M} \times \underbrace{\left|\frac{\sin(\pi\varepsilon_k)}{\pi\varepsilon_k}\right|}_{\cong 1-\frac{\pi^2\varepsilon_k^2}{6}}. \end{aligned} \quad (10)$$

We know that $J_k^M\cdot\left(1-\frac{\pi^2\epsilon^2}{6}\right) < z_k^M < J_k^M$. Note that in an OFDMA uplink with an adaptive power control for each user, the averaged SNR of each user is identical; i.e., $J_1^M = J_2^M = \cdots = J_K^M = \bar{\mathcal{J}}^M = \sqrt{3\mu_3(M)\times\frac{9\mathrm{SNR}}{\pi^2\epsilon^2\mathrm{SNR}+9}}$. We find the Cumulative Distribution Function (CDF) is

$$\begin{aligned} F_M(z) &= \Pr\left\{z_k^M \le z\right\} \\ &= 1-\Pr\left\{\varepsilon_k^2 \le \frac{6(\bar{\mathcal{J}}^M - z)}{\pi^2\bar{\mathcal{J}}^M}\right\} \\ &= 1-\frac{\sqrt{6(\bar{\mathcal{J}}^M - z)}}{\pi\epsilon\sqrt{\bar{\mathcal{J}}^M}}, \end{aligned} \quad (11)$$

and the PDF to be

$$f_M(z) = \frac{\partial F_M(z)}{\partial z} = \begin{cases} \frac{3}{\pi\epsilon\sqrt{6\bar{\mathcal{J}}^M(\bar{\mathcal{J}}^M - z)}} & \bar{\mathcal{J}}^M\left(1 - \frac{\pi^2\epsilon^2}{6}\right) < z < \bar{\mathcal{J}}^M. \\ 0 & \text{otherwise.} \end{cases} \tag{12}$$

From (6), for an OFDMA uplink with each subcarrier modulated by M-ary square QAM, the averaged BER can be represented as

$$P_{BER}^M = \mu_1(M)\int_{\bar{\mathcal{J}}^M\cdot\left(1-\frac{\pi^2\epsilon^2}{6}\right)}^{\bar{\mathcal{J}}^M} \operatorname{erfc}(z) f_M(z)\,\mathrm{d}\,z + \mu_2(M)\int_{\bar{\mathcal{J}}^M\cdot\left(1-\frac{\pi^2\epsilon^2}{6}\right)}^{\bar{\mathcal{J}}^M} \operatorname{erfc}(3z) f_M(z)\,\mathrm{d}\,z. \tag{13}$$

The function erfc(z) can be represented as an infinite series [12, page 939], and as a result,

$$\begin{aligned}\int_{\bar{\mathcal{J}}^M\cdot\left(1-\frac{\pi^2\epsilon^2}{6}\right)}^{\bar{\mathcal{J}}^M} \operatorname{erfc}(z) f_z(z)\,\mathrm{d}\,z &= 1 - \frac{2\sqrt{6}}{\pi\epsilon\sqrt{\pi\bar{\mathcal{J}}^M}}\sum_{n=1}^{\infty}\frac{(-1)^{n+1}\mathcal{D}_n^M}{(2n-1)(n-1)!} \\ &= 1 - \frac{2\sqrt{6}}{\pi\epsilon\sqrt{\pi\bar{\mathcal{J}}^M}}\sum_{n=1}^{\infty}\beta_{1,n}^M,\end{aligned} \tag{14}$$

and

$$\int_{\bar{\mathcal{J}}^M\cdot\left(1-\frac{\pi^2\epsilon^2}{6}\right)}^{\bar{\mathcal{J}}^M} \operatorname{erfc}(3z) f_M(z)\,\mathrm{d}\,z = 1 - \frac{2\sqrt{6}}{\pi\epsilon\sqrt{\pi\bar{\mathcal{J}}^M}}\sum_{n=1}^{\infty}\beta_{2,n}^M, \tag{15}$$

where $\mathcal{D}_n^M = \int_0^{\pi\epsilon\sqrt{\frac{\bar{\mathcal{J}}^M}{6}}} (\bar{\mathcal{J}}^M - y^2)^{2n-1}\mathrm{d}\,y$, $\beta_{1,n}^M = \frac{(-1)^{n+1}}{(2n-1)(n-1)!}\cdot\mathcal{D}_n^M$ and $\beta_{2,n}^M = 3^{2n-1}\beta_{1,n}^M = \frac{(-1)^{n+1}3^{2n-1}}{(2n-1)(n-1)!}\cdot\mathcal{D}_n^M$. Therefore, (13) can be rewritten as

$$P_{BER}^M = \frac{2\sqrt{M}-3}{\sqrt{M}\log_2\sqrt{M}} - \frac{2\sqrt{6}(\sqrt{M}-1)}{\pi\epsilon\log_2\sqrt{M}\sqrt{M\pi\bar{\mathcal{J}}^M}}\sum_{n=1}^{\infty}\beta_{1,n}^M - \frac{2\sqrt{6}(\sqrt{M}-2)}{\pi\epsilon\log_2\sqrt{M}\sqrt{M\pi\bar{\mathcal{J}}^M}}\sum_{n=1}^{\infty}\beta_{2,n}^M. \tag{16}$$

The coefficients $\mathcal{D}_n^M$, $\beta_{1,n}^M$ and $\beta_{2,n}^M$ can be iteratively defined as follows:

$$\begin{aligned}\mathcal{D}_n^M &= \int_0^{\pi\epsilon\sqrt{\frac{\bar{\mathcal{J}}^M}{6}}} (\bar{\mathcal{J}}^M - y^2)^{2n-1}\mathrm{d}\,y \\ &= \pi\epsilon\sqrt{\frac{\bar{\mathcal{J}}^M}{6}}\left(\bar{\mathcal{J}}^M - \frac{\pi^2\epsilon^2\bar{\mathcal{J}}^M}{6}\right)^{2n-1} - 2(2n-1)\cdot\mathcal{D}_n^M \\ &\quad + \frac{2(2n-1)\bar{\mathcal{J}}^M\pi\epsilon\sqrt{\frac{\bar{\mathcal{J}}^M}{6}}\left(\bar{\mathcal{J}}^M - \frac{\pi^2\epsilon^2\bar{\mathcal{J}}^M}{6}\right)^{2n-2}}{4n-3} \\ &\quad + \frac{2(2n-1)(2n-2){\bar{\mathcal{J}}^M}^2}{4n-3}\cdot\mathcal{D}_{n-1}^M.\end{aligned} \tag{17}$$

By resolving (17), we can represent $\mathcal{D}_n^M$ and $\beta_{1,n}^M$ as

$$\begin{aligned}\mathcal{D}_n^M &= \frac{\pi\epsilon\sqrt{\frac{\bar{\mathcal{J}}^M}{6}}\left(\bar{\mathcal{J}}^M - \frac{\pi^2\epsilon^2\bar{\mathcal{J}}^M}{6}\right)^{2n-1}}{4n-1} \\ &\quad + \frac{2(2n-1)\pi\epsilon\sqrt{\frac{\bar{\mathcal{J}}^M}{6}}\bar{\mathcal{J}}^M\left(\bar{\mathcal{J}}^M - \frac{\pi^2\epsilon^2\bar{\mathcal{J}}^M}{6}\right)^{2n-2}}{(4n-1)(4n-3)} \\ &\quad + \frac{4(2n-1)(2n-2){\bar{\mathcal{J}}^M}^2}{(4n-1)(4n-3)}\cdot\mathcal{D}_{n-1}^M,\end{aligned} \tag{18}$$

and

$$\begin{aligned}\beta_{1,n}^M &= \frac{(-1)^{n+1}\pi\epsilon\sqrt{\frac{\bar{\mathcal{J}}^M}{6}}\left(\bar{\mathcal{J}}^M - \frac{\pi^2\epsilon^2\bar{\mathcal{J}}^M}{6}\right)^{2n-1}}{(2n-1)(4n-1)(n-1)!} \\ &\quad + \frac{2(-1)^{n+1}\pi\epsilon\sqrt{\frac{\bar{\mathcal{J}}^M}{6}}\bar{\mathcal{J}}^M\left(\bar{\mathcal{J}}^M - \frac{\pi^2\epsilon^2\bar{\mathcal{J}}^M}{6}\right)^{2n-2}}{(4n-1)(4n-3)(n-1)!} \\ &\quad - \frac{8(2n-3){\bar{\mathcal{J}}^M}^2}{(4n-1)(4n-3)}\cdot\beta_{1,n-1}^M.\end{aligned} \tag{19}$$

Define a_n^M and b_n^M, respectively, as

$$a_n^M = \frac{(-1)^{n+1}\pi\epsilon\sqrt{\frac{\bar{\mathcal{J}}^M}{6}}\left(\bar{\mathcal{J}}^M - \frac{\pi^2\epsilon^2\bar{\mathcal{J}}^M}{6}\right)^{2n-1}}{(2n-1)(4n-1)(n-1)!}, \tag{20a}$$

$$b_n^M = \frac{2(-1)^{n+1}\pi\epsilon\sqrt{\frac{\bar{\mathcal{J}}^M}{6}}\bar{\mathcal{J}}^M\left(\bar{\mathcal{J}}^M - \frac{\pi^2\epsilon^2\bar{\mathcal{J}}^M}{6}\right)^{2n-2}}{(4n-1)(4n-3)(n-1)!}. \tag{20b}$$

Then (20) can be rewritten as

$$a_n^M = \frac{(-1)(2n-3)(4n-5)\left(\bar{\mathcal{J}}^M - \frac{\pi^2\epsilon^2\bar{\mathcal{J}}^M}{6}\right)^2}{(n-1)(2n-1)(4n-1)}\cdot a_{n-1}^M, \tag{21a}$$

$$b_n^M = \frac{(-1)(4n-5)(4n-7)\left(\bar{\mathcal{J}}^M - \frac{\pi^2\epsilon^2\bar{\mathcal{J}}^M}{6}\right)^2}{(n-1)(4n-1)(4n-3)}\cdot b_{n-1}^M. \tag{21b}$$

Therefore, (19) can be simplified as

$$\begin{aligned}\beta_{1,n}^M &= a_n^M + b_n^M - \frac{8(2n-3){\bar{\mathcal{J}}^M}^2}{(4n-1)(4n-3)}\cdot\beta_{1,n-1}^M \\ &= \frac{(-1)(2n-3)(4n-5)\left(\bar{\mathcal{J}}^M - \frac{\pi^2\epsilon^2\bar{\mathcal{J}}^M}{6}\right)^2}{(n-1)(2n-1)(4n-1)}\cdot a_{n-1}^M \\ &\quad + \frac{(-1)(4n-5)(4n-7)\left(\bar{\mathcal{J}}^M - \frac{\pi^2\epsilon^2\bar{\mathcal{J}}^M}{6}\right)^2}{(n-1)(4n-1)(4n-3)}\cdot b_{n-1}^M \\ &\quad - \frac{8(2n-3){\bar{\mathcal{J}}^M}^2}{(4n-1)(4n-3)}\cdot\beta_{1,n-1}^M.\end{aligned} \tag{22}$$

Appendix B
BER with Gaussian Frequency Offsets

Assume that $\varepsilon_k \sim \mathcal{N}(0, \sigma_\epsilon^2)$, the averaged BER is given by

$$P_{BER}^M \cong \mu_1(M)\cdot\mathbb{E}\left\{\operatorname{erfc}\left(z_k^M\right)\right\} + \mu_2(M)\cdot\mathbb{E}\left\{\operatorname{erfc}\left(3z_k^M\right)\right\}, \tag{23}$$

where

$$\mathbb{E}\left\{\operatorname{erfc}\left(z_k^M\right)\right\} = 1 - \frac{2}{\sqrt{\pi}} \sum_{n=1}^{\infty} \frac{(-1)^{n+1}\left(J_k^M\right)^{2n-1}}{(2n-1)(n-1)!} \cdot \underbrace{\int_{-\infty}^{\infty} \left(1 - \frac{\pi^2 \varepsilon_k^2}{6}\right)^{2n-1} \frac{1}{\sqrt{2\pi}\sigma_\epsilon} e^{-\frac{y^2}{2\sigma_\epsilon^2}} \mathrm{d}\,y}_{\mathcal{D}_{2n-1}^M} \tag{24}$$

and

$$\mathbb{E}\left\{\operatorname{erfc}\left(3z_k^M\right)\right\} = 1 - \frac{2}{\sqrt{\pi}} \sum_{n=1}^{\infty} \frac{(-1)^{n+1}\left(3J_k^M\right)^{2n-1}}{(2n-1)(n-1)!} \cdot \mathcal{D}_{2n-1}^M. \tag{25}$$

We can easily find that

$$\mathcal{D}_{2n-1}^M = \left(1 - \frac{(4n-3)\pi^2\sigma_\epsilon^2}{6}\right)\mathcal{D}_{2n-2}^M + \frac{(4n-4)\pi^2\sigma_\epsilon^2}{6}\mathcal{D}_{2n-3}^M, \tag{26a}$$

$$\mathcal{D}_{2n-2}^M = \left(1 - \frac{(4n-5)\pi^2\sigma_\epsilon^2}{6}\right)\mathcal{D}_{2n-3}^M + \frac{(4n-6)\pi^2\sigma_\epsilon^2}{6}\mathcal{D}_{2n-4}^M. \tag{26b}$$

REFERENCES

[1] A. Tonello, N. Laurenti, and S. Pupolin, "Analysis of the uplink of an asynchronous multi-user DMT OFDMA system impaired by time offsets, frequency offsets, and multi-path fading," in *Proc. IEEE Veh. Technol. Conf. (VTC)*, vol. 3, Sept. 2000, pp. 1094-1099.

[2] D. Kivanc, G. Li, and H. Liu, "Computationally efficient bandwidth allocation and power control for OFDMA," *IEEE Trans. Wireless Commun.*, vol. 2, no. 6, pp. 1150-1158, Nov. 2003.

[3] I. C. Wong and B. L. Evans, "Optimal OFDMA subcarrier, rate, and power allocation for ergodic rates maximization with imperfect channel knowledge," in *Proc. IEEE Int. Conf. Acoustics, Speech, Signal Processing (ICASSP)*, vol. 3, Honolulu, HI, Apr. 2007.

[4] L. Rugini and P. Banelli, "BER of OFDM systems impaired by carrier frequency offset in multipath fading channels," *IEEE Trans. Wireless Commun.*, vol. 4, no. 5, pp. 2279-2288, Sept. 2005.

[5] Z. Zhang, W. Jiang, H. Zhou, Y. Liu, and J. Gao, "High accuracy frequency offset correction with adjustable acquisition range in OFDM systems," *IEEE Trans. Wireless Commun.*, vol. 4, no. 1, pp. 228-237, Jan. 2005.

[6] M.-O. Pun, M. Morelli, and C.-C. Kuo, "Maximum-likelihood synchronization and channel estimation for ofdma uplink transmissions," *IEEE Trans. Commun.*, vol. 54, no. 4, pp. 726-736, Apr. 2006.

[7] Z. Cao, U. Tureli, and Y.-D. Yao, "Deterministic multiuser carrier-frequency offset estimation for interleaved OFDMA uplink," *IEEE Trans. Commun.*, vol. 52, no. 9, pp. 1585 – 1594, Sept. 2004. [Online]. Available: http://dx.doi.org/10.1109/TCOMM.2004.833183

[8] D. Huang and K. Letaief, "An interference-cancellation scheme for carrier frequency offsets correction in OFDMA systems," *IEEE Trans. Commun.*, vol. 53, no. 7, pp. 1155-1165, July 2005.

[9] K. Cho and D. Yoon, "On the general BER expression of one- and two-dimensional amplitude modulations," *IEEE Trans. Commun.*, vol. 50, no. 7, pp. 1074-1080, July 2002.

[10] Z. Zhang, W. Zhang, and C. Tellambura, "Robust OFDMA uplink synchronization by exploiting the variance of carrier frequency offsets," *IEEE Trans. Veh. Technol.*, vol. 57, no. 5, pp. 3028-3039, Sept. 2008.

[11] D. Tse and P. Viswanath, *Fundamentals of Wireless Communication*. Cambridge University Press, 2005.

[12] I. S. Gradshteyn and I. M. Ryzhik, *Table of Integrals, Series, and Products*, 5th ed. Academic Press, Inc., 1994.

Zhongshan Zhang received the M.S. degree in computer science in 2001 and Ph.D. degree in electrical engineering in 2004 from the Beijing University of Posts and Telecommunications (BUPT). From Aug. 2004 he joined DoCoMo Beijing Laboratories as an associate researcher, and was promoted to be a researcher in Dec. 2005. From Feb. 2006, he joined University of Alberta, Edmonton, AB, Canada, as a postdoctoral fellow. His main research interests include statistical signal processing, synchronization and channel estimation in Multiple-input Multiple-output (MIMO) orthogonal frequency division multiplexing (OFDM) systems, and cooperative communications.

Chintha Tellambura (SM'02) received the B.Sc. degree (with first-class honors) from the University of Moratuwa, Moratuwa, Sri Lanka, in 1986, the M.Sc. degree in electronics from the University of London, London, U.K., in 1988, and the Ph.D. degree in electrical engineering from the University of Victoria, Victoria, BC, Canada, in 1993.

He was a Postdoctoral Research Fellow with the University of Victoria (1993-1994) and the University of Bradford (1995-1996). He was with Monash University, Melbourne, Australia, from 1997 to 2002. Presently, he is a Professor with the Department of Electrical and Computer Engineering, University of Alberta. His research interests include Diversity and Fading Countermeasures, Multiple-Input Multiple-Output (MIMO) Systems and Space-Time Coding, and Orthogonal Frequency Division Multiplexing (OFDM).

Prof. Tellambura is an Associate Editor for the IEEE TRANSACTIONS ON COMMUNICATIONS and the Area Editor for Wireless Communications Systems and Theory in the IEEE TRANSACTIONS ON WIRELESS COMMUNICATIONS. He was Chair of the Communication Theory Symposium in Globecom'05 held in St. Louis, MO.